UNIWERSYTET TECHNOLOGICZNO-PRZYRODNICZY
IM. JANA I JĘDRZEJA ŚNIADECKICH W BYDGOSZCZY
ZESZYTY NAUKOWE NR 260
TELEKOMUNKACJA I ELEKTRONIKA 15 (2011), 49-61

MRI IMAGE ANALYSIS IN PATIENTS WITH A TUMOR OF THE CENTRAL NERVOUS SYSTEM – AN ATTEMPT OF DEVELOPING A MANAGEMENT ALGORITHM

Maciej Śniegocki[1], Agnieszka Nowacka[2], Jacek Fisz[3]
Aleksandra Śniegocka[4], Marcin Buczkowski[5]

[1] Department of Neurotraumatology CM UMK

[2] Department of Neurosurgery and Neurotraumatology CM UMK

[3] Department of Computer Science and Methodology of Science Work CM UMK

[4] Department of Clinical Psychology CM UMK
University Hospital No. 1, ul. M. Skłodowskiej-Curie 9, 85-094 Bydgoszcz

[5] Department of Physics and Biophysics UWM,
Plac Cieszyński 1 (bl. 43), 10-726 Olsztyn

Summary: Magnetic resonance imaging study is currently the reference method for the detection and diagnosis of the central nervous system tumors. A large number of tumors, especially high-grade, has a higher water content in the cells, which results in prolongation of MRI T1 and T2 what appearance as increased signal intensity in in T2-weighted images and the reduction in T1-weighted images. MRI can be performed with administration of contrast agent, which shortens T1 and increases signal on T1-weighted sequences. This allows to identify areas of increased angiogenesis), which is the exponent of the cancer malignancy degree and its biological activity. Obtained MRI images are analyzed and evaluated by a radiologist and a clinician. Most of the time it is the "by the eye" analysis, which is based on the MRI image evaluation by the generally accepted radiological standards. However, this method is relatively inaccurate. which in turn can bring to the wrong diagnosis of the disease and implementation or even lack of implementation of appropriate treatment. More and more researches are conducted in this area, but developed methods are usually very complicated and difficult to carry out by the "layman" which is the clinician. That is why the attempt is made, to develop a simple and clear algorithm for MRI image analysis in patients with the central nervous system tumors, allowing for quick and objective evaluation of magnetic resonance imaging study.

Keywords: tumor, MRI image, angiogenesis, image analysis

1. TUMORS OF THE CENTRAL NERVOUS SYSTEM

Central nervous system tumors are approximately 1.5% of all cancers occurring in the human body, but their incidence is still increasing. Globally, the incidence of deaths due to intracranial tumors is estimated to be approximately 2.3% of all deaths due to cancer. 70-75% of them are primary tumors, and 20-25% are metastatic tumors. Due to the specific structure and functions of the brain, central nervous system tumors differ

significantly from tumors located in other parts of the body. The very location of the tumor, regardless of its growth and malignancy, affects on the prognosis and patient's functional status. In case of location of the lesion in the area of important vital structures, both a tumor growth and its surgical treatment is a huge risk of severe disability or death of the patient.

Tumors of the central nervous system can be classified according to several basic criteria. The first one is the presentation of tumors due to their location within the cranial cavity. There are supratentorial tumors (located in the lobes of the brain, in deep structures of the telencephalon and diencephalon), which are 80-85% of all intracranial tumors in adults, and 40% in children, and infratentorial tumors (located within the cerebellum, brainstem, or the cerebellopontine angle), representing 15-20% of intracranial tumors in adults and 60% in children. This division is based on images obtained in radiological examinations, such as conventional radiography (X-ray), computed tomography (CT), magnetic resonance imaging (MRI) or positron emission tomography (PET). It is widely used in clinical practice, mainly because the location of the pathology is responsible for the occurrence of specific neurological symptoms, and allows to determine the quality of possible damage of the central nervous system after the surgery. Another criterion of division of the central nervous system tumors is the origin of the tumor tissue, first introduced by the World Health Organization (WHO) in 1979. The latest, 2007, WHO classification accounts the current state of knowledge about the biology of cancer, intracellular regulatory pathways, disturbed in the process of oncogenesis, and aspects of the therapeutic methods prediction.

TUMORS OF NEUROEPITHELIAL TISSUE

Astrocytic tumours
Pilocytic astrocytoma
- Pilomyxoid astrocytoma

Subependymal giant cell astrocytoma
Pleomorphic xanthoastrocytoma
Diffuse astrocytoma
- Fibrillary astrocytoma
- Gemistocytic astrocytoma
- Protoplasmic astrocytoma

Anaplastic astrocytoma
Glioblastoma
- Giant cell glioblastoma
- Gliosarcoma

Gliomatosis cerebri

Oligodendroglial tumours
Oligodendroglioma
Anaplastic oligodendroglioma

Oligoastrocytic tumours
Oligoastrocytoma
Anaplastic oligoastrocytoma

Ependymal tumours
Subependymoma
Myxopapillary ependymoma
Ependymoma
- Cellular
- Papillary
- Clear cell
- Tanycytic

Anaplastic ependymoma

Choroid plexus tumours
Choroid plexus papilloma
Atypical choroid plexus papilloma
Choroid plexus carcinoma

Other neuroepithelial tumours
Astroblastoma
Choroid glioma of the third ventricle
Angiocentric glioma

Neuronal and mixed neuronal-glial tumours
Dysplastic gangliocytoma of cerebellum (Lhermitte-Duclos)
Desmoplastic infantile astrocytoma/ganglioglioma
Dysembryoplastic neuroepithelial tumour
Gangliocytoma
Ganglioglioma
Anaplastic ganglioglioma
Central neurocytoma
Extraventricular naurocytoma
Cerebellar liponeurocytoma
Papillary glioneuronal tumour [PGNT]
Rosette-forming glioneuronal tumour of the fourth ventricle
Paraganglioma

Tumours of the pineal region
Pineocytoma
Pineal parenchymal tumour of intermediate differentiation
Pineoblastoma
Papillary tumour of the pineal region [PTPR]

Embryonal tumours
Medulloblastoma
- Desmoplastic/nodular medulloblastoma
- Medulloblastoma with extensive nodularity
- Anaplastic medulloblastoma
- Large cell medulloblastoma

CNS primitive neuroectodermal tumour
- CNS Neuroblastoma
- CNS Ganglioneuroblastoma
- Medulloepithelioma
- Ependymoblastoma

Atypical teratoid/rhabdoid tumour

TUMOURS OF CRANIAL AND PARASPINAL NERVES

Schwannoma (neurilemoma, neurinoma)
- Cellular
- Plexiform
- Melanotic

Neurofibroma
- Plexiform

Perineurinoma
- Perineurinoma, NOS
- Malignant perineurinoma

Malignant peripheral nerve sheath tumour (MPNST)
- Epithelioid MPNST
- MPNST with mesenchymal differentiation
- Melanotic MPNST
- MPNST with glandular differentiation

TUMOURS OF THE MENINGES

Tumours of meningothelial cells
Meningioma
- Meningothelial
- Fibrous (fibroblastic)
- Transitional (mixed)
- Psammomatous
- Angiomatous
- Microcystic
- Secretory
- Lymphoplasmacyte-rich
- Metaplastic
- Chordoid
- Clear cell
- Atypical
- Papillary
- Rhabdoid
- Anaplastic (malignant)

Mesenchymal tumours
Lipoma
Angiolipoma
Hibernoma
Liposarcoma
Solitary fibrous tumour
Fibrosarcoma
Malignant fibrous histiocytoma
Leiomyoma
Leiomyosarcoma
Rhabdomyoma
Rhabdomyosarcoma
Chondroma
Chondrosarcoma
Osteoma
Osteosarcoma
Osteochondroma
Haemangioma
Epithelioid haemangioendothelioma
Haemangiopericytoma
Anaplastic haemangiopericytoma
Angiosarcoma
Kaposi sarcoma
Ewing sarcoma (PNET)

Primary melanocytic lesions
Diffuse melanocytosis
Melanocytoma
Malignant melanoma
Meningeal melanomatosis

Other neoplasms related to the meninges
Haemangioblastoma

LYMPHOMAS AND HAEMATOPOIETIC NEOPLASMS

Malignant lymphomas
Plasmocytoma
Granulocytic sarcoma

GERM CELL TUMOURS

Germinoma
Embryonal carcinoma
Yolk sac tumour
Choriocarcinoma
Teratoma
- Mature
- Immature
- Teratoma with malignant transformation

Mixed germ cell tumour

TUMOURS OF THE SELLAR REGION

Craniopharyngioma
- Adamantinomatous
- Papillary

Granular cell tumour
Pituicytoma
Spindle cell oncocytoma of the adenohypophysis

METASTATIC TUMOURS

Fig. 1. Classification of the central nervous system tumors according to WHO, 2007.

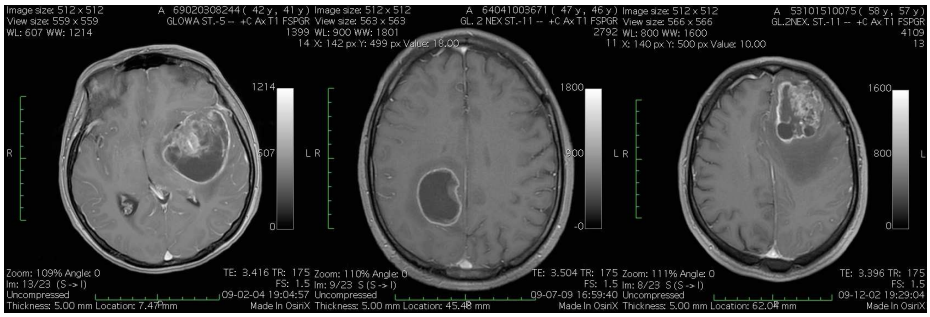
Image size: 512 x 512
View size: 559 x 559
WL: 607 WW: 1214
A 69020308244 (42 y , 41 y)
GLOWA ST.-5 -- +C Ax T1 FSPGR
1399
Zoom: 109% Angle: 0
Im: 13/23 (S -> I)
Uncompressed
09-02-04 19:04:57
Thickness: 5.00 mm Location: 7.47 mm
TE: 3.416 TR: 175
FS: 1.5
Made In OsiriX
1214
607
0
R
L R
Image size: 512 x 512
View size: 563 x 563
WL: 900 WW: 1801
14 X: 142 px Y: 499 px Value: 18.00
A 64041003671 (47 y , 46 y)
GL. 2 NEX ST.-11 -- +C Ax T1 FSPGR
2792
Zoom: 110% Angle: 0
Im: 9/23 S (S -> I)
Uncompressed
09-07-09 16:59:40
Thickness: 5.00 mm Location: 45.48 mm
TE: 3.504 TR: 175
FS: 1.5
Made In OsiriX
1800
900
-0
L R
Image size: 512 x 512
View size: 566 x 566
WL: 800 WW: 1600
11 X: 140 px Y: 500 px Value: 10.00
A 53101510075 (58 y , 57 y)
GL.2NEX, ST.-11 -- +C Ax T1 FSPGR
4109
13
Zoom: 111% Angle: 0
Im: 8/23 S (S -> I)
Uncompressed
09-12-02 19:29:04
Thickness: 5.00 mm Location: 62.04 mm
TE: 3.396 TR: 175
FS: 1.5
Made In OsiriX
1600
800
0
L

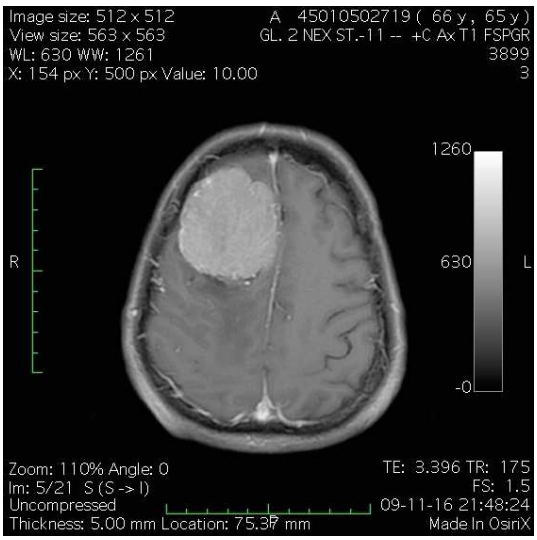
Image size: 512 x 512
View size: 563 x 563
WL: 630 WW: 1261
X: 154 px Y: 500 px Value: 10.00
A 45010502719 (66 y , 65 y)
GL. 2 NEX ST.-11 -- +C Ax T1 FSPGR
3899
3
1260
630
-0
R
L
Zoom: 110% Angle: 0
Im: 5/21 S (S -> I)
Uncompressed
Thickness: 5.00 mm Location: 75.3
TE: 3.396 TR: 175
FS: 1.5
09-11-16 21:48:24
Made In OsiriX

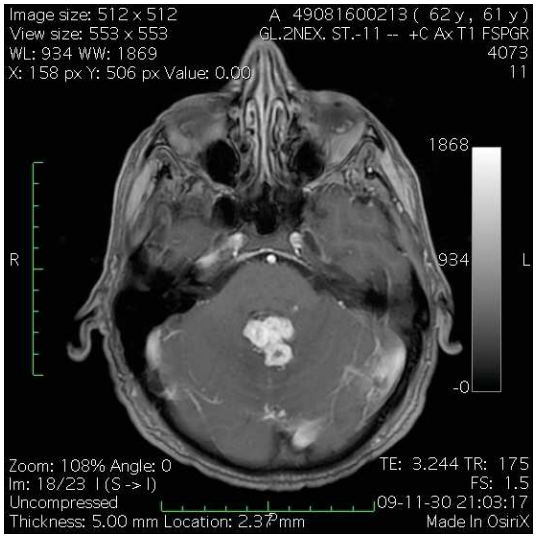
Image size: 512 x 512
View size: 553 x 553
WL: 934 WW: 1869
X: 158 px Y: 506 px Value: 0.00
A 49081600213 (62 y , 61 y)
GL.2NEX. ST.-11 -- +C Ax T1 FSPGR
4073
11
1868
934
-0
R
L
Zoom: 108% Angle: 0
Im: 18/23 I (S -> I)
Uncompressed
Thickness: 5.00 mm Location: 2.37 mm
TE: 3.244 TR: 175
FS: 1.5
09-11-30 21:03:17
Made In OsiriX

rearranges relatively to the magnetic field lines. Then they are stimulated by the resonant frequent electromagnetic pulses. During the stimulation decay, occurs an emission of a radio frequency waves. Received signals differ by intensity, depending on the type of tissue from which they originate. A large number of tumors, especially high-grade, has a higher water content in the cells, which results in prolongation of MRI T1 and T2 what appearace as increased signal intensity in in T2-weighted images and the reduction in T1-weighted images.

Table 2. Type of MRI signal in the case of selected central nervous system tumors.

Tumor histological type	T1 – weighted images	T2 – weighted images
Low grade gliomas	hipo/-izointensive	hiperintensive
High grade gliomas	hipo/-izointensive	hiperintensive
Meningiomas	iso-/hipointensive	iso-/hipointensive
Metastatic tumors	hipo/-izointensive	hiperintensive

As with CT, MRI can be performed without or with administration of contrast agent (usually gadolinium), which shorten T1 and increase signal on T1-weighted sequences. This allows to identify areas of increased blood flow (increased angiogenesis). Increased angiogenesis, the formation of blood vessels in tumor tissues, is the exponent of the cancer malignancy degree and its biological activity. Microcirculation can be illustrated by examination of brain tissue perfusion (eg. PWI MRI – weighted perfusion MRI, DCE MRI - dynamic contrast enchanced MRI). Administration of the contrast agent can also detect damage to the blood-brain barrier and allows to find the boundary between tumor and surrounding edema. The degree of after-contrast signal increasement depends on the concentration of contrast agent and magnetic fields force.

There are many MRI sequences and techniques, eg. FLAIR – fluid attenuated inversion recovery, STIR – short tau inversion recovery, MRA – magnetic resonance angiography, DWI – difussion weighted imaging, MRS – magnetic resonance spectroscopy, DTT MRI – difussion tensor tractography MRI. This an examination highly exceed computed tomography in the diagnosis of tumors of the central nervous system. Of course it has its limitations, such as the relatively long examinating time, sensitivity to motion artifacts, lack of examination possibility in case of the metal presence in patient's body, and the high price of examination. Despite that, it has many advantages, that put it in the first place in neuroimaging diagnosis, including:

- the possibility of obtaining images in any plane, which allows to define a very precise topographical relationships in relation to adjacent anatomical structures,
- high contrast resolution between imaging tissues,
- lack of bone artifacts,
- greater sensitivity than CT,
- possibility to conduct the examination in pregnant women (very low risk of adverse effects on the fetus of the magnetic field, as opposed to harmful ionizing radiation X in the case of CT),
- non-invasive examination,
- repeatability of examination.

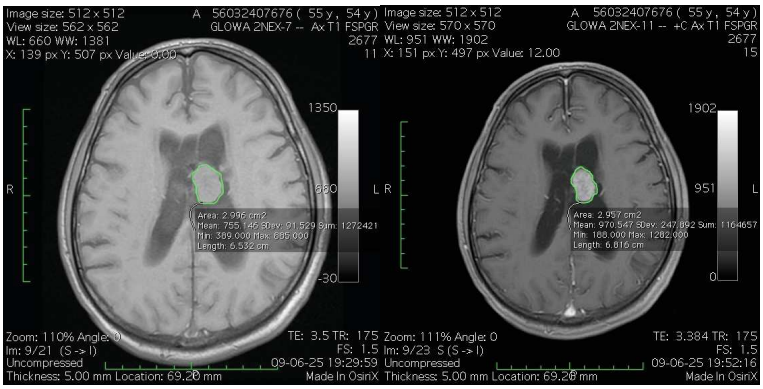
Image size: 512 x 512
View size: 562 x 562
WL: 660 WW: 1381
X: 139 px Y: 507 px Value: 9.00
A 56032407676 (55 y, 54 y)
GLOWA 2NEX-7 -- Ax T1 FSPGR
2677
11
1350
660
-30
R
L R
Area: 2.995 cm2
Mean: 755.146 Sdev: 91.529 Sum: 1272421
Min: 389.000 Max: 995.000
Length: 6.532 cm
Zoom: 110% Angle: 0
Im: 9/21 (S -> I)
Uncompressed
Thickness: 5.00 mm Location: 69.20 mm
TE: 3.5 TR: 175
FS: 1.5
09-06-25 19:29:59
Made In OsirixX
Image size: 512 x 512
View size: 570 x 570
WL: 951 WW: 1902
X: 151 px Y: 497 px Value: 12.00
A 56032407676 (55 y, 54 y)
GLOWA 2NEX-11 -- +C Ax T1 FSPGR
2677
15
1902
951
0
L R
L
Area: 2.957 cm2
Mean: 970.547 Sdev: 247.992 Sum: 1164657
Min: 188.000 Max: 1282.000
Length: 6.816 cm
Zoom: 111% Angle: 0
Im: 9/23 S (S -> I)
Uncompressed
Thickness: 5.00 mm Location: 69.20 mm
TE: 3.384 TR: 175
FS: 1.5
09-06-25 19:52:16
Made In OsirixX

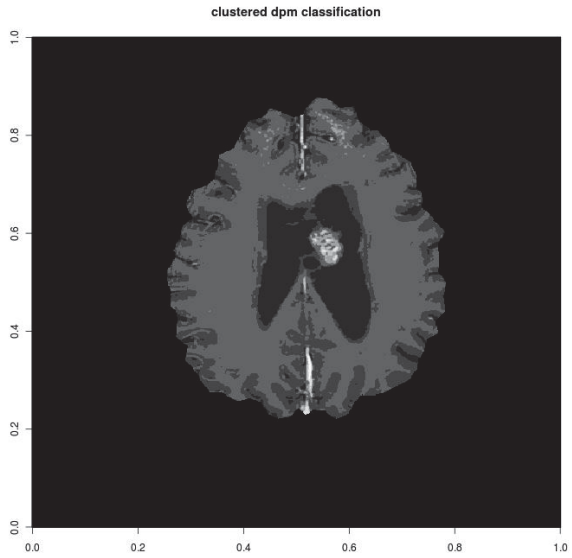
clustered dpm classification
0.0
0.2
0.4
0.6
0.8
1.0

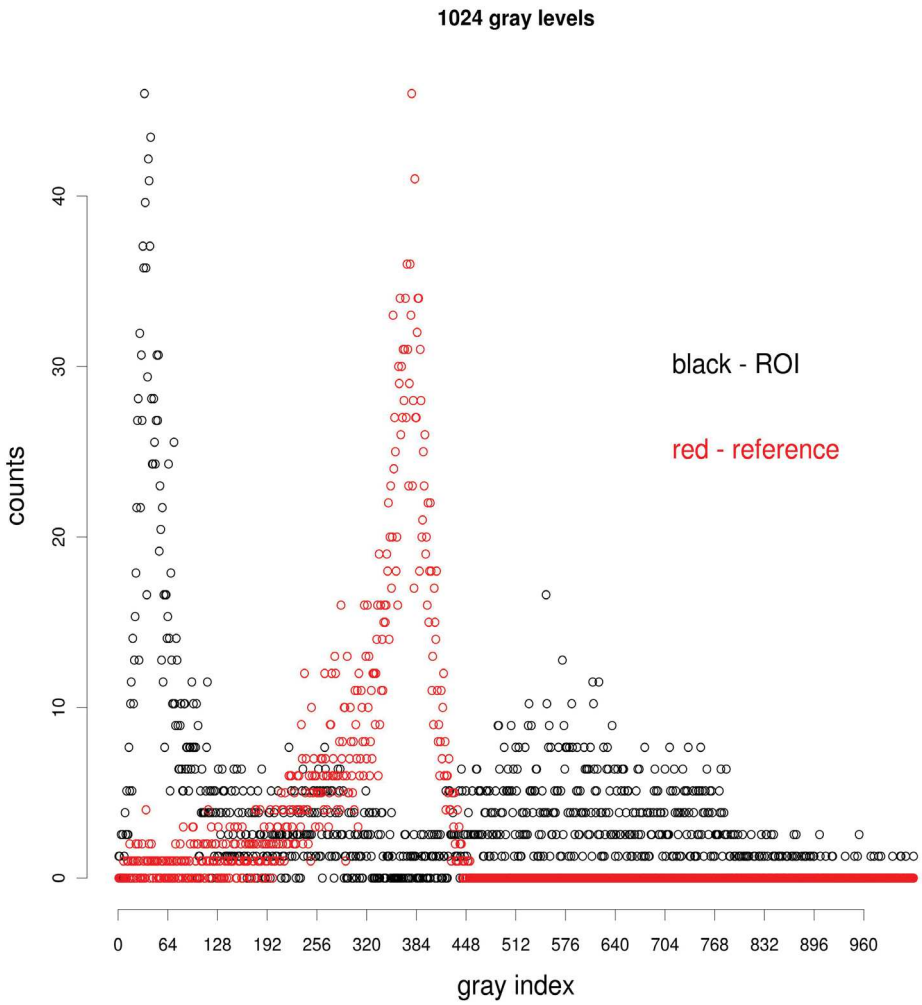
1024 gray levels
counts
0
10
20
30
40
black - ROI
red - reference
0
64
128
192
256
320
384
448
512
576
640
704
768
832
896
960
gray index

The new method can help to facilitate the work of both radiologists – the assessment of MRI images, and clinicians – when planning treatment, monitoring the disease and predicting prognosis for patient survival. Due to its simplicity and fast, direct obtaining of concrete results, it can also be used by those less experienced in the analysis of magnetic resonance images.

BIBLIOGRAPHY

[1] Aksoy F.G., Lev M.H., 2000. Dynamic Contrast − Enhanced Brain Perfusion Imaging: Technique and Clinical Applications. Sem Ultrasound CT MRI, 21 (6), pp. 462-477.
[2] Al-Okaili R.N., Krejza J., Woo J.H., Wolf R.L., O'Rourke D.M., Judy K.D., Poptani H., Melhem E.R., 2007. Intraaxial brain masses: MR imaging–based diagnostic strategy – initial experience. Radiology 243, pp. 539-550.
[3] Aronen H.J., Gazit I.E., Louis D.N., Buchbinder B.R., Pardo F.S., Weisskoff R.M., Griffith R.H., Cosgrove G.R., Halpern E.F., Hochberg F.H., Rosen B.R., 1994. Cerebral Blood Volume Maps of Gliomas: Comparison with Tumor Grade and Histologic Findings. Radiology 191, pp. 41-51.
[4] Brem S., Cotran R., Folkman J., 1972. Tumor angiogenesis: a quantitative method for histologic grading. J Natl Cancer Inst 48, pp. 347-356.
[5] Emblem K.E., Zoellner F.G., Tennoe B., Nedregaard B., Nome T., Due-Tonnessen P., Hald J.K., Scheie D., Bjornerud A., 2008. Predictive modeling in glioma grading from MR perfusion images using support vector machines. Magn Reson Med 60, pp. 945-952.
[6] Folkman J., 1992. The role of angiogenesis in tumor growth. Semin Cancer Biol, 3, pp. 65-71.
[7] Folkman J., 1990. What is the evidence that tumors are angiogenesis dependent? J Natl Cancer Inst 82, pp. 4-6.
[8] Ginsberg L., Fuller G., Schomer D., Kau B.A., Kispert D.B., 1996. Does lack of enhancement of brain tumors on MR imaging correlate with low grade malignancy? A histopathologic study. [In:] Proceedings of the American Society of Neuroradiology, Seattle–Washington, pp. 32-33.
[9] Glotsos D., Tohka J., Ravazoula P., Cavouras D., Nikiforidis G., 2005. Automated diagnosis of brain tumors astrocytomas using probabilistic neural network clustering and support vector machines. Int J Neural Syst 15, pp. 1-11.
[10] Greenberg M.S., Arredonto N., 2010. Handbook of neurosurgery – 7th edition, Thieme.
[11] Higano S., Yun X., Kumabe T., Watanabe M., Mugikura S., Umetsu A., Sato A., Yamada T., Takahashi S., 2006. Malignant astrocytic tumors: clinical im- portance of apparent diffusion coefficient in prediction of grade and prognosis. Radiology 241, pp. 839-846.
[12] Huang Y., Lisboa P.J.G., El-Deredy W., 2003. Tumour grading from magnetic resonance spectroscopy: a comparison of feature extraction with variable selection. Stat Med 22, pp. 147-164.
[13] Knopp E.A., Cha S., Johnson G., Mazumdar A., Golfinos J.G., Zagzag D., Miller D.C., Kelly P.J., Kricheff I.I., 1999. Glial Neoplasms: Dynamic Contrast − Enhanced T2* − weighted MR Imaging. Radiology 211, pp. 791-798.

[14] Kremer S., Grand S., Remy C., Esteve F., Lefournier V., Pasquier B., Hoffmann D., Benabid A.L., Le Bas J.F., 2002. Cerebral blood volume mapping by MR imaging in the initial evaluation of brain tumors. J Neuroradiol 29, pp. 105-113.
[15] Law M., Cha S., Knopp E. A., Johnson G., Arnett J., Litt A.W., 2002. High−Grade Gliomas and Solitary metastases: Diffe − rentiation by Using Perfusion and Proton Spectroscopic MR Imaging. Radiology 222, pp. 715-721.
[16] Lev M.H., Hochberg F., 1998. Perfusion Magnetic Resonance Imaging to Assess Brain Tumor Responses to New Therapies. Cancer Control 5 (2), pp. 115-123.
[17] Lev M.H., Ozsunar Y., Henson J.W., Rasheed A.A., Barest G.D., Harsh G.R., Fitzek M.M., Chiocca E.A., Rabinov J.D., Csavoy A.N., Rosen B.R., Hochberg F.H., Schaefer P.W., Gonzalez R.G., 2004. Glial tumor grading and outcome prediction using dynamic spin-echo MR susceptibility mapping com- pared with conventional contrast-enhanced MR: confounding effect of elevated rCBV of oligodendrogliomas. Am J Neuroradiol 25, pp. 214-221.
[18] Liberski P.P., Kozubski W., Biernat W., Kordek R., 2011. Neuroonkologia kliniczna. Wyd. Czelej.
[19] Louis D.N., Ohgaki H., Wiestler O.D., Cavenee W.K., Burger P.C., Jouvet A., Scheithauer B.W., 2007. The 2007 WHO Classification of Tumours of the Central Nervous System. Springer-Verlag.
[20] Lüdemann L., Grieger W., Wurm R., Budzisch M., Hamm B., Zimmer C., 2001. Comparison of dynamic contrast−enhanced MRI with WHO tumor grading for gliomas. Eur Radiol 11, pp. 1231-1241.
[21] Majo´s C., Julia`-Sape´ M., Alonso J., Serrallonga M., Aguilera C., Acebes J.J., Aru´s C., Gili J., 2004. Brain tumor classification by proton MR spectroscopy: comparison of diagnostic accuracy at short and long TE. Am J Neuro-radiol 25, pp. 1696-1704.
[22] Melhem E.R., Davatzikos C., 2008. Multi-parametric tissue characterization of brain neoplasms and their recurrence using pattern classification of MR images. Acad Radiol 15, pp. 966-977.
[23] Østergaard L., Hochberg F.H., Rabinov J.D., Sorensen A.G., Lev M., Kim L., Weisskoff R.M., Gonzalez R.G., Gyldensted C., Rosen B.R., 1999. Early changes measured by magnetic resonance imaging in cerebral blood flow, blood volume, and blood–brain barrier permeability following dexamethasone treatment in patients with brain tumors. J Neurosurg 90, pp. 300-305.
[24] Principi M., Italiani M., Guiducci A., Aprile I., Muti M., Giulianelli G., Ottoviano P., 2003. Perfusion MRI in the evaluation of the relationship between tumour growth, necrosis and angiogenesis in glioblastomas and grade 1 meningiomas. Neuroradiology 45, pp. 205-211.
[25] Provenzale J.M., Mukundan S., Baroriak D.P., 2006. Diffusion-weighted and perfusion MR imaging for brain tumor characterization and assessment of treatment. Radiology 239, pp. 632-649.
[26] Provenzale J.M., Mukundan S., Baroriak D.P., 2006. Diffusion-weighted and perfusion MR imaging for brain tumor characterization and assessment of treatment response. Radiology 239, pp. 632-649.
[27] Provenzale J.M., Wang G.R., Brenner T., Petrella J.R., Sorensen A.G., 2002. Comparison of Permeability in High−Grade and Low−Grade Brain Tumors Using Dynamic Susceptibility Contrast MR Imaging. Am J Roentgenol 178, pp. 711-716.

[28] Roberts H.C., Roberts T.P.L., Brasch R.C., Dillon W.P., 2000. Quantitative measurement of microvascular permeability in human brain tumors achieved using dynamic contrast − enhanced MR imaging: correlation with histologic grade. Am J Neuroradiol 21, pp. 891-899.
[29] Roberts H.C., Roberts T.P.L., Lee T.Y., Dillon W.P., 2002. Dynamic Contrast − Enhanced CT of Human Brain Tumors: Quantitative Assessment of Blood Volume, Blood Flow, and Microvascular Permeability: Report of Two Cases. Am J Neuroradiol 23, pp. 828-832.
[30] Siegal T., Rubinstein R.I., Tzuk-Shina T., Gomori J.M., 1997. Utility of relative cerebral blood volume mapping derived from perfusion magnetic resonance imaging in the routine follow up of brain tumors. J Neurosurg 86, pp. 22-27.
[31] Smith S.M., Jenkinson M., Woolrich M.W., Beckmann C.F., Behrens T.E., Johansen-Berg H., Bannister P.R., De Luca M., Drobnjak I., Flitney D.E., Niazy R.K., Saunders J., Vickers J., Zhang Y., De Stefano N., Brady J.M., Matthews P.M., 2004. Advances in functional and structural MR image analysis and implementation as FSL. Neuroimage 23 (suppl 1).
[32] Sugahara T., Korogi Y., Kochi M., Ikushima I., Hirai T., Okuda T., Shigematsu Y., Liang L., Ge Y., Ushio Y., Takahashi M., 1998. Correlation of MR Imaging − Determinated Cerebral Blood Maps with Histologic and Angiographic Determination of Vascularity of Gliomas. Am J Roengenol 171, pp. 1479-1486.
[33] Walecki J., Chojnacka E., 2007. Diagnostyka obrazowa guzów wewnątrz-czaszkowych – część I – guzy neuroepitelialne. Onkologia w praktyce klinicznej, tom 3, nr 4, pp. 177-197.
[34] Weber M.A., Zoubaa S., Schlieter M., Juttler E., Huttner H.B., Geletneky K., Ittrich C., Lichy M.P., Kroll A., Debus J., Giesel F.L., Hartmann M., Essig M., 2006. Diagnostic performance of spectroscopic and perfusion MRI for distinc- tion of brain tumors. Neurology 66, pp. 1899-1906.
[35] Young R.J., Knopp E.A., 2006. Brain MRI: tumor evaluation. J Magn Reson Imaging 24, pp. 709-724.
[36] Zacharaki E.I., Wang S., Chawla S., Wolf R., Melhem E.R., Davatzikos C., 2009. Classification of brain tumor type and grade using MRI texture and shape in a machine learning scheme. Magnetic Resonance in Medicine 62, pp. 1609-1618.
[37] Zimny A., Sąsiadek M., 2005. Badania perfuzyjne TK i MR – nowe narzędzie w diagnostyce guzów wewnątrzczaszkowych. Adv Clin Exp Med. 14; 3, pp. 583-592.

ANALIZA OBRAZU MRI U CHORYCH Z GUZEM OŚRODKOWEGO UKŁADU NERWOWEGO – PRÓBA OPRACOWANIA ALGORYTMU POSTĘPOWANIA

Streszczenie

Badanie metodą rezonansu magnetycznego jest aktualnie metodą referencyjną przy wykrywaniu i diagnozowaniu nowotworów centralnego układu nerwowego. Duża część nowotworów, zwłaszcza o wysokim stopniu złośliwości, charakteryzuje się większą zawartością wody w komórkach, co w badaniu MRI skutkuje wydłu-żeniem T1 i T2, uwidocznionym jako nasilenie sygnału w obrazach T2-zależnych oraz jego obniżeniem w obrazach T1-zależnych. MRI można przeprowadzić

z podaniem środka kontrastowego, co powoduje skrócenie czasu T1 i podniesienie sygnału w sekwencjach T1-zależnych. Pozwala to zidentyfikować obszary wzmożonej angiogenezy, która jest wykładnikiem stopnia złośliwości nowotworu oraz jego aktywności biologicznej. Otrzymane obrazy MRI są analizowane oraz oceniane przez radiologa, a następnie klinicystę. Najczęściej jest to analiza „na oko" i opiera się ona na ocenie obrazu MRI z ogólnie przyjętymi normami radiologicznymi. Jest to jednak metoda stosunkowo niedokładna, co sprawia, iż otrzymane obrazy MRI mogą zostać ocenione w sposób niewłaściwy, co z kolei może przyczynić się do postawienia złej diagnozy co do choroby pacjenta i wdrożenie lub wręcz brak wdrożenia odpowiedniego leczenia. Prowadzonych jest coraz więcej badań w zakresie wprowadzenia skomputeryzowanego algorytmu służącego do oceny badania MRI, jednak wypracowane metody są najczęściej bardzo skomplikowane i trudne do przeprowadzenia przez „laika" jakim jest klinicysta. Właśnie dlatego podjęta została próba opracowania w miarę prostego i czytelnego algorytmu analizy obrazu MRI u pacjentów z chorobą nowotworową centralnego układu nerwowego, która pozwoli na szybką i obiektywną ocenę badania rezonansu magnetycznego.

Słowa kluczowe: nowotwory, obrazowanie MRI, angiogeneza, analiza obrazu